Measurement of Forces between Hydroxypropylcellulose Polymers: Temperature Favored Assembly and Salt Exclusion

Cecile Bonnet-Gonnet,† Sergey Leikin, Sulene Chi,‡ Donald C. Rau,* and V. Adrian Parsegian

Laboratory of Physical and Structural Biology, National Institute of Child Health and Human Development, National Institutes of Health, Bethesda, Maryland 20892-0924

Received: July 18, 2000; In Final Form: November 21, 2000

The thermodynamic forces between hydroxypropylcellulose (HPC) molecules at close separation have been measured using the osmotic stress method coupled with X-ray scattering. Two force regimes are apparent: a very short ranged, temperature insensitive force that dominates interactions within the last 2.5 Å separation and a longer-ranged force that varies exponentially vs distance with a decay length of about 3−4 Å. The longer-ranged force characteristics are strikingly similar to those found for many other macromolecules. We have previously argued that these characteristics are due to a hydration or water structuring force. The amplitude of the longer ranged force in these condensed arrays decreases linearly with temperature. The force switches from repulsive to attractive at ∼40 °C, about the same temperature at which HPC precipitates from dilute solution. The entropy of the HPC condensed array, derived from the temperature dependence of the force, also varies exponentially vs spacing with a 3−4 Å decay length. Measured forces are also surprisingly sensitive to added salt. Salt acts by its exclusion from the HPC phase. The salt concentration gradient within the space between polymers, inferred from the salt concentration dependence of the force curves, is itself apparently exponential with the about same 3−4 Å decay length as the force and entropy.

Introduction

Hydroxypropylcellulose (HPC) belongs to a class of single-chain flexible polysaccharides whose water-solution properties are industrially important and useful[1,2] but scientifically puzzling. Paradoxically, insoluble cellulose is made soluble by adding nominally hydrophobic hydroxypropyl groups. At room-temperature HPC dissolves to 40 wt % then forms a second liquid-crystalline phase. Heated above about 40 °C, however, even dilute HPC solutions precipitate to this same liquid-crystal phase.[3−7] The nature of the condensed liquid-crystalline phase formed above 40 °C and the forces that create it have not been adequately examined.

We have now measured the forces between HPC polymers at close distances. The thermodynamics of concentrated macromolecular arrays can be examined using the osmotic stress technique[8] that precisely controls the chemical potentials of water and other small molecules that are in equilibrium with the condensed phase. This measurement of changes in free energy of the macromolecular phase is not possible with the gravimetric mixtures used to construct phase diagrams. In the osmotic stress experiment, a solution of a polymer that is excluded from condensed arrays of macromolecules, such as poly(ethylene glycol) (PEG), is used to create a bathing reservoir of known polymer osmotic pressure. The activities of all other components in the polymer solution that can exchange with the condensed phase (H^+, salt, and other small solutes) and temperature are held fixed. If the macromolecular array is sufficiently ordered to allow measurement of the interaxial spacing by X-ray scattering, then the outward osmotic stress of the array is known as a function of distance.

These thermodynamic forces can be due either to direct interactions between macromolecules, e.g., electrostatic, van der Waals, or hydration forces, or to changes in the configurational free energies of the macromolecule in the concentrated phase. Because force is a spatial derivative of free energy and entropy is the temperature derivative of free energy, the sensitivity of these forces to temperature allows one to calculate entropy versus separation. The dependence of the pressure−distance curves on the activities of other small molecules, for example, salt, that can exchange between the PEG solution and macromolecular array gives the partitioning of these solutes between the bulk solution and the condensed phase. Osmotic stress has proven a powerful tool for dissecting the thermodynamics of many condensed systems.[9−11]

Direct measurement of the thermodynamic forces between HPC polymers in condensed arrays shows two distinct regimes in the last 10 Å of separation between surfaces, i.e., in the Bragg spacing range between 10.9 Å seen for dry HPC and 20 Å. For Bragg spacings between ∼12.5 and 20 Å, the distance dependence of the interaction can be adequately described by an exponential with a 3−4 Å decay length. The characteristics of this force are qualitatively very similar to the interactions seen between many other macromolecules, both charged and uncharged, in water, as, for example, DNA, xanthan, schizophyllan, collagen, and many lipid bilayers (see, e.g., Leikin et al.[9]). At spacings even closer than about 2.5 Å, the forces between HPC polymers change very rapidly with intermolecular distance.

While the very short ranged force and the decay length of the longer ranged force are insensitive to temperature, the coefficient of the longer ranged force decreases dramatically

* Corresponding author: Bldg. 9, Rm 1E−122, National Institutes of Health, Bethesda, MD 20892-0924. Tel 301-402-4698. Fax 301-402-9462. E-mail *donrau@helix.nih.gov*.

† Present address: Rhodia, Coatings Applicability Laboratory, 52 rue de la Haie-Coq, 3308 Aubervilliers Cedex, France.

‡ Present address: Duke University School of Medicine, Duke University Medical Center, PO Box 28649, Durham, NC 27701.

10.1021/jp002531f
Published on Web 01/26/2001

with increasing temperature. The force curves show a smooth variation from repulsion at low temperatures to attraction with a transition temperature at ~40 °C for these condensed arrays (at an estimated macromolecular concentration of ~300−500 mg/mL). This temperature is just slightly below the cloud point temperature (~42 °C) for the precipitation of HPC from dilute solution (0.03 mg/mL).

Added salt lowers the cloud-point transition temperature even though HPC is nominally uncharged. By monitoring the change in bulk salt concentration as dry samples are hydrated, we find that salt is excluded from the HPC condensed phase. Salt is acting indirectly on HPC precipitation through its exclusion. By analyzing the changes in osmotic stress force curves with salt concentration as excess, salt osmotic pressures, we can estimate the salt concentration in the condensed phase as a function of HPC spacing.

Materials and Methods

Sample Preparation and Equilibration. Hydroxypropylcellulose was purchased from Polysciences, Inc. The polymer used had an average molecular weight of 60 000 and an average of ~3 hydroxypropyl groups incorporated per glucose unit. It was used without further purification. HPC was dissolved in 10 mM TrisCl (pH 7.5), 4 mM EDTA at a concentration of ~2% (w/w) and then concentrated to a transparent, solid film by slow dialysis in a Pierce Microdialysis System 500 cell with a 1000 MW cutoff membrane against a 40% (w/w) solution of poly(ethylene glycol) (MW ~8000) in water. Five films (~6 mm in diameter and 0.5−1 mm thick) were formed simultaneously and cut into small (1 × 2 mm) samples that were used for the force measurements.

The force−distance curves were measured using the osmotic stress technique coupled with X-ray scattering.[8,9] Solid samples were equilibrated against excess solutions of 10 mM TrisCl (pH 7.5), 2 mM EDTA, and poly(ethylene glycol) (8000 or 20 000 MW PEG from Fluka) at various temperatures. Some equilibrating solutions also included various concentrations of NaCl. The comparatively large PEG molecules are excluded from the HPC films and compete osmotically for the available water. No difference in force−distance curves was observed using 8000 or 20 000 MW PEG, confirming that these polymers are excluded from the HPC pellets. The osmotic pressure Π contribution of the PEG in the bathing solution concentrates the HPC phase in much the same way as a semipermeable piston pushing on the polysaccharide solution with a mechanical pressure Π.

To achieve osmotic pressures above $10^{8.2}$ dyn/cm^2 (~200 atm), salt-free samples were suspended above saturated salt solutions (avoiding direct contact) in tightly sealed tubes and were equilibrated against the water vapor in equilibrium with the salt solution. The relative humidity of the vapor was varied using saturated solutions of different inorganic salts.[12] Equivalent osmotic pressures were calculated from tabulated relative humidities.[13]

X-ray Scattering. For the X-ray scattering experiments, the samples after equilibration were sealed with a small amount of the equilibrating solution (or vapor) in specially designed X-ray cells described elsewhere.[14] The cells were mounted into temperature-controlled holders, and Bragg reflections were measured using a fixed anode X-ray generator, cameras, and imaging system as described in Kuznetsova et al.[15] Spacings in the 10−20 Å region can be determined with an accuracy of 0.2−0.4 Å.

Cloud Point Measurements. The precipitation temperature (cloud point) of dilute HPC solutions was determined by optical turbidity measurement. The HPC solutions, ranging in concentration from 0.03 to 0.4 mg/mL, were placed in quartz cuvettes with path lengths varying between 1 and 10 mm, depending on concentration. Optical absorbances at wavelengths varying between 350 and 500 nm, depending on HPC concentration, were obtained using a Shimadzu UV-2101PC spectrophotometer and were recorded as a function of the solution temperature during slow heating and cooling cycles controlled using a programmable Neslab model RTE 111 refrigerated bath/circulator. Temperature was monitored using a scanning thermocouple thermometer (Cole-Parmer model 92800−00) equipped with a quick-response Teflon PFA-insulated microprobe (Cole-Parmer E−08506−70) placed directly in a control cuvette filled with water and mounted next to the HPC sample.

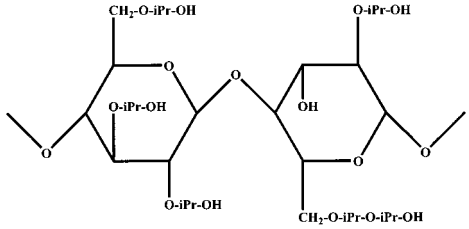

Figure 1. Schematic representation of the chemical structure of hydroxypropylcellulose. The average degree of substitution is ~3 hydroxypropyl groups per glucose monomer.

Salt Partitioning. The partitioning of NaCl and water between bulk solution and a condensed HPC phase was measured from the changes in the refractive indices of salt solutions equilibrated against initially dry samples of HPC. Dry HPC was equilibrated against various weights of a 2 molal NaCl solution at 45 °C. The refractive index of the bathing solution was measured using an Abbe C-10 refractometer at 20 °C before and after the equilibration of the sample. As a control, we observed no change in the refractive index of pure water after equilibration with HPC at 45 °C; the dry polysaccharide does not contain any significant soluble components that could affect the refractive index of the bathing solution. A change in the refractive index after solvation of a dry sample indicates a change in the bathing solution salt concentration due to a preferential exclusion (an increase in the bathing solution refractive index) or inclusion (decrease) of salt in the macromolecular sample compared with water.

Results

X-ray Scattering. The chemical structure of HPC is illustrated in Figure 1. The average degree of substitution of hydroxypropyl groups is ~3 per saccharide. The hydroxyl groups both of the glucose and of the hydroxypropyl group itself can be substituted. Figure 2a shows a typical pattern for the low-angle X-ray scattering from a thick (~0.5−1 mm) condensed HPC film, equilibrated against 30% (w/w) PEG (8000 MW) in 10 mM TrisCl/2 mM EDTA (pH 7.5) at 20 °C (Π_{PEG} = 7.36). We have not succeeded in forming arrays of sufficient order to allow indexing the unit cell from the higher order reflections and determining the polymer packing symmetry. Occasionally samples were well enough ordered to give oriented scattering (two arcs) but still with no observable higher order scattering. The integrated radial intensity profile of the powder pattern scattering is shown in the Figure 2b. The peak position was determined by a quadratic fit to the peak after subtracting the contribution from a constant background (a straight line after radial integration).

Figure 3 shows the dependence of the average Bragg spacing, D_{Br}, between HPC molecules on the osmotic pressure, Π, at 10

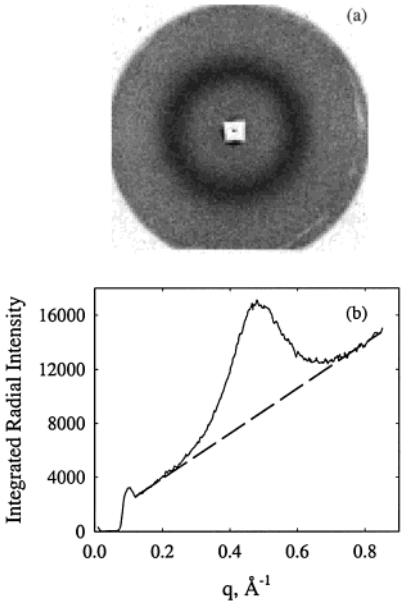

Figure 2. (a) Typical X-ray scattering pattern of condensed HPC equilibrated against 30% PEG (~8000 MW) in 10 mM TrisCl (pH 7.5), 2 mM EDTA and at 20 °C. The radially integrated scattering intensity is shown in (b) as a function of the wave vector $q = (4\pi/\lambda)\sin(\vartheta/2)$, where λ is the wavelength of Cu Kα X-rays and $\vartheta/2$ is the scattering angle.

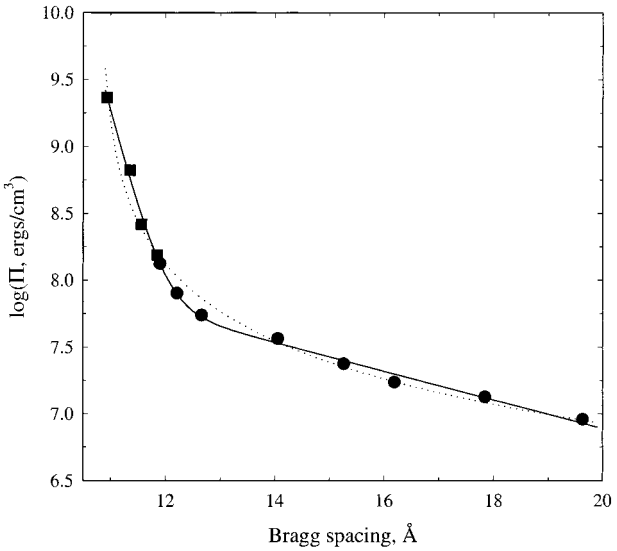

Figure 3. Osmotic pressure of PEG in bathing solution plotted against the interaxial Bragg spacing characterizing the separation of polymers in the HPC condensed phase at 10 °C. The circle (●) and square (■) symbols represent HPC films equilibrated against bathing PEG solutions or against vapor pressures of saturated salt solutions, respectively. Essentially dry HPC (equilibrated against 10% relative humidity) gives a Bragg spacing of 10.9 Å. Each point represents the equilibrium spacing at which the osmotic pressure is balanced by the repulsive force between HPC molecules. This thermodynamic force includes contributions from both direct interactions and configurational entropy. The dotted line shows a power law fit to the force curve, whereas the solid line shows the fit to a double exponential function. Fitting parameters are given in the text.

°C. HPC films were equilibrated against bathing PEG solutions for the low-pressure data and against the vapor pressure of saturated salt solutions for the high-pressure data. The two methods overlap at log(Π) ~8.2. For Bragg spacings larger than ~15−16 Å, the powder pattern scattering becomes increasingly diffuse and completely disappears at log(Π) < 6.9 or D_{Br} ~20 Å. Samples still remain phase separated from the PEG (8000 MW) solution, however, down to log(Π) ~6.5. At even lower osmotic pressures, the samples completely dissolve into the PEG solution.

The osmotic pressure applied by PEG solution concentrates the HPC phase acting against a repulsive intermolecular force that can be due either to soft potential interactions between molecules or to changes in configurational entropy as the molecules are condensed. We assume that the X-ray diffraction peaks give Bragg spacings of crystalline (translationally ordered) structures. Then, if the molecular packing symmetry that relates Bragg spacings to intermolecular distances (D_{int}) and to volumes is known, the free energy of concentrating the HPC phase can be calculated from the osmotic pressure. Although we do not know the symmetry, the factor that connects D_{Br} to D_{int} is typically close to unity for parallel polymers. For example, this factor is $2/\sqrt{3}$ (~1.155) for the commonly observed hexagonal packing of polymer chains.[16] We have assumed that Bragg spacings are reasonably close estimates of intermolecular distances. If we further assume that the volume/chain scales as D_{Br}^2, i.e., that the distance between all neighboring rods changes in proportion, then the data shown in Figure 3 can be used to estimate the changes in free energy as HPC chains are brought closer together.

The thermodynamic force shown in Figure 3 appears to show two distinct regimes, with a fairly sharp bend in log(Π) versus D_{Br} data at D_{Br} ~12.5 Å. At 10% relative humidity (log(Π) = 9.5), the Bragg spacing is 10.9 Å, which we take as the limiting spacing for HPC. Thermodynamic force curves are often analyzed as a power law, assuming that the change in configurational entropy dominates polymer interactions as macromolecules are concentrated. The dashed line in Figure 3 is the fit of the data to the functional form

$$\Pi = \frac{C}{(D_{Br} - D_0)^n} \quad (1)$$

where the spacing of the dry HPC, D_0, is assumed to be the limiting spacing of 10.9 Å. The best fitting parameters (with a coefficient of determination, r^2, of 0.945) are: $c = (1.2 \pm 0.2) \times 10^8$ and $n = 1.04 \pm 0.08$. The fit for this functional form is sensitive to the choice of D_0. A somewhat better fit ($r^2 = 0.982$) is obtained for $D_0 = 10.8$ Å with fitting parameters $c = (1.7 \pm 0.1) \times 10^8$ and $n = 1.35 \pm 0.06$. Considering only hard shell configurational entropy of the chains (no soft potentials), the exponent n is expected to vary between 2 and 3 for flexible, closely packed linear polymers.[17,18]

Because exponentially varying forces have been observed with many macromolecular arrays, we also fit the data (solid line in Figure 3) by a double exponential function of the form

$$\Pi = \mathrm{A}\exp(-(D_{Br} - D_0)/\lambda_1) + \mathrm{B}\exp(-(D_{Br} - D_0)\lambda_2) \quad (2)$$

D_0, the "dry" Bragg spacing, is again taken as 10.9 Å. For this functional form, the choice of D_0 determines only the magnitudes of the force amplitudes, A and B, but has no effect on the quality of the fit itself. The best fitting parameters to the data ($r^2 = 0.997$) are: $\mathrm{A} = (2.5 \pm 0.2) \times 10^9$ ergs/cm^3; $\mathrm{B} = (7.3 \pm 1.0) \times 10^7$ ergs/cm^3; $\lambda_1 = 0.28 \pm 0.01$ Å; and $\lambda_2 = 4.0 \pm 0.3$ Å. The longer ranged $\lambda_2 \sim 4$ Å decay length exponential is very similar to the force curves observed for many other macromolecules.[9]

Force Curves; Effect of Temperature. Pressure-distance curves measured between 5 °C and 60 °C are shown in Figure 4. These results clearly indicate that the observed curves are

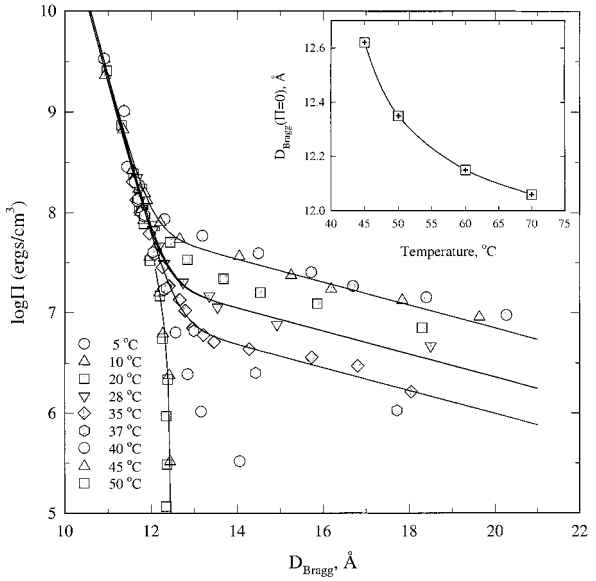

Figure 4. HPC force curves for nine temperatures ranging from 5 to 50 °C. All curves appear to converge at high stresses (log(Π) greater than about 8) to a temperature insensitive force. The amplitude of the force at lower stresses decreases significantly with increasing temperature. Double exponential fits (eq 2) are shown for the force curves at 10, 28, 35, and 50 °C. Only the amplitude of the longer ranged force, $B(T)$, was allowed to vary in these fits; the values of the shorter ranged force amplitude (log(A) = 9.51) and decay length (λ_1 = 0.27 Å) and the longer ranged force decay length (λ_2 = 3.8 Å) were fixed, as described in the text. The temperature dependence of the equilibrium spacing $D_{Br}^{\Pi_{PEG}=0}$ (with no applied PEG stress) is shown in the figure inset. Even though the shorter-ranged force is insensitive to temperature, HPC polymers continue to move closer in the absence of PEG as the temperature is increased from 45 to 70 °C. The amplitude of the attractive force must continue to increase over this temperature range.

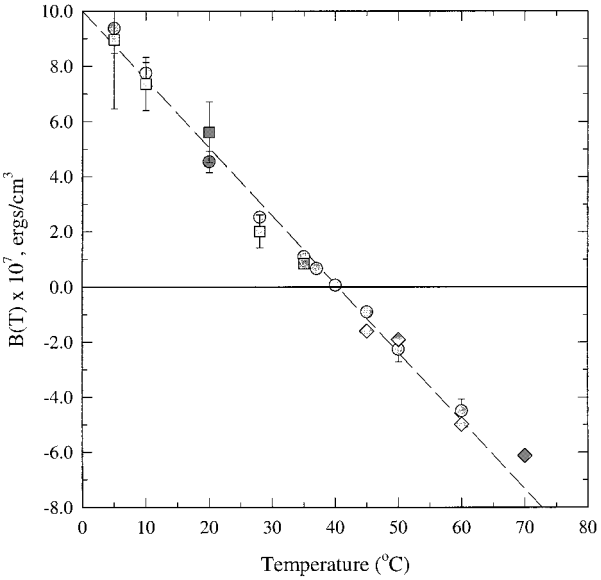

Figure 5. Amplitude of the longer ranged exponential, $B(T)$, as a function of temperature. The square symbols (■) show the amplitudes and standard errors calculated from fits to a double exponential function (eq 2) allowing the amplitudes and decay lengths of both the longer ranged and shorter ranged force to vary. The circles (●) show the longer ranged force amplitudes and standard errors from fits to a double exponential function allowing only $B(T)$ to vary (A, λ_1, and λ_2 are held fixed). The diamonds (♦) show $B(T)$ estimated from the equilibrium spacings with no applied PEG stress at temperatures above ∼40 °C, assuming a balance of the repulsive shorter ranged and attractive longer ranged exponential forces (eq 3). Again, only $B(T)$ is allowed to vary. The longer ranged force amplitude varies approximately linearly with temperature. The linear fit including all estimates of the longer ranged force amplitude gives $B(T) = (9.81 \pm 0.25) \times 10^7 - (2.42 \pm 0.06) \times 10^6$ T. The transition from repulsive to net attractive force occurs at 40.5 ± 0.5 °C.

indeed the sum of at least two distinct forces with different characteristic lengths. Under high osmotic stress (log(Π) > 8), the data at the different temperatures converge to a common curve. At lower stresses, the spacing at a fixed pressure depends strongly on temperature. Repulsion weakens as the temperature is increased. Above ∼40 °C, the longer-ranged force is net attractive. HPC arrays remain condensed, with a measurable Bragg spacing, without any applied PEG osmotic pressure. An increase in the magnitude of the attractive force between HPC molecules for temperatures above 40 °C can be inferred from the decrease in Bragg spacing with no applied PEG osmotic stress, D_{Br}^0, as temperature increases (Figure 4 inset). This attraction is taken to work against the shorter-ranged temperature-independent repulsion.

Although the data are not sufficiently precise to resolve unambiguously the functional forms of the underlying attractive and repulsive component forces, the force data sets at 5, 10, 20, and 35 °C cover a sufficiently wide range of separations such that fits to the double exponential function (eq 2) used in Figure 3 are well determined. The amplitudes and decay lengths of both the short-ranged and long-ranged forces were allowed to vary, and D_0 again was taken as 10.9 Å. The average amplitude, A, and decay length, λ_1, of the shorter-ranged force over this temperature range are $(2.8 \pm 0.7) \times 10^9$ ergs/cm^3 and = 0.26 ± 0.03 Å, respectively. A single exponential fit of the common, shorter ranged force using only the high-pressure (log(Π) > 8.0) data collected at all temperatures gives closely similar parameters, with an amplitude $A = (3.2 \pm 0.7) \times 10^9$ erg/cm^3 and a decay length λ_1 = 0.27 ± 0.02 Å. The best-fit decay lengths of the longer ranged force, λ_2, were 3.8 ± 0.4, 4.0 ± 0.3, 3.6 ± 0.5, and 4.2 ± 0.8 Å, respectively, at 5, 10, 20, and 35 °C. Both decay lengths appear to be insensitive to temperature, at least over this 25° range. In contrast, the best fitting amplitudes of the longer ranged force depend strongly

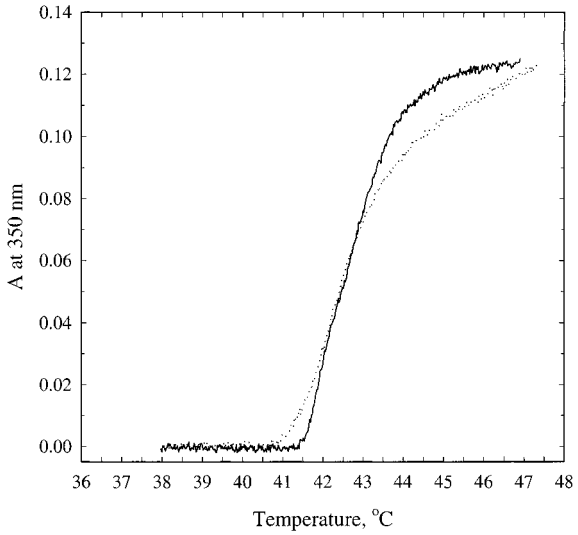

Figure 6. Change in optical absorbance (turbidity) at 350 nm for the slow (0.025 °C/min) heating (solid line) and cooling (dotted line) of a dilute HPC solution (0.003%, 30 μg/mL). At this heating rate, the clouding transition is insensitive to HPC concentration at least to 0.3%. The precipitation of HPC from dilute solution occurs at an approximate temperature only 1−2 °C higher than seen for the transition between repulsive and attractive forces in very concentrated HPC condensed arrays (∼500 mg/mL).

on temperature, varying from $(9.0 \pm 2.5) \times 10^7$ erg/cm^3 at 5 °C to (0.8 ± 0.2) 10^7 erg/cm^3 at 35 °C.

The data over the entire temperature range can be well described by a double exponential function by varying only the temperature-dependent amplitude of the longer-ranged force, $B(T)$, while assuming constant (temperature independent) values for the shorter ranged force amplitude ($A = 3.2 \times 10^9$), and decay length ($\lambda_1 = 0.27$ Å) and for the longer ranged force decay length ($\lambda_2 = 3.8$ Å). The solid lines in Figure 4 show fits to the data at 10, 28, 35, and 50 °C.

Figure 5 shows several estimates of the longer ranged force amplitude, $B(T)$, as a function of temperature. Amplitudes from double exponential fits to the 5−35 °C data sets, allowing all four parameters, A, B(T), λ_1, and λ_2, to vary, are shown by the squares. Longer ranged force amplitudes from double exponential fits to the data sets at all temperatures with fixed values of A, λ_1, and λ_2 are shown by the circles. Additionally, the attractive amplitude of the longer-ranged force, $B(T)$, can also be estimated from the Bragg spacing, D^0_{Br}, observed in the absence of PEG stress at temperatures above ∼40 °C (Figure 4 inset). The diamonds in Figure 5 show these amplitudes calculated assuming a balance of the two exponential forces at the equilibrium distance,

$$B(T) = A\frac{\exp(-(D^0_{Br} - D_0)/\lambda_1)}{\exp(-(D^0_{Br} - D_0)/\lambda_2)} \qquad (3)$$

using the values for A, λ_1, and λ_2 given above. The particular choice of D_0 affects the calculation of $B(T)$ only as a scaling factor.

The striking feature of the plot in Figure 5 is the approximately linear dependence of force amplitude on temperature. With increasing temperature, this force component changes from repulsive to attractive with a transition temperature at ∼40.5 °C.

Self-Assembly from Dilute Solution. The transition from net repulsion to attraction seen in condensed arrays of HPC is also apparent in the precipitation of HPC from dilute solution with increasing temperature. Figure 6 shows the optical absorbance (turbidity) at 350 nm of a 0.03 mg/mL HPC solution as a function of temperature for slow heating and cooling (∼0.025 °C/min).

The onset of aggregation between 40 and 42 °C seen by the rapid increase in absorbance agrees with the observations of others[3−7] who used HPC with similar degrees of substitution. The inflection point is independent of heating rate between 0.025 and 0.1 °C/min and of HPC concentration between 0.03 and 0.4 mg/mL. Heating rates faster than about 0.5 °C/min do show a delay in the onset of the aggregation, suggesting that the heating curve is affected by reaction kinetics. The rate-independent cooling curve represents either equilibrium or spinodal conditions. Even though a small hysteresis in turbidity is apparent, it is clear that the self-assembly of HPC from dilute solution and the transition from net repulsion to attraction in condensed arrays occur at about the same temperature.

Thermodynamic Analysis. We can use the measured temperature-dependent Π-D_{Br} curves in Figure 4 to extract thermodynamic potentials of the condensed HPC phase. With the reservation that the specific packing geometry and chain conformation are not precisely known, the volume of the water/disaccharide unit in this phase can be estimated from the Bragg spacing. The resulting Π-V curves can be integrated to give a packing free energy change as a function of spacing (eq A5 of the appendix). The entropy and, consequently, the enthalpy can be extracted from the temperature dependence of the free energy. In practice, the entropy can be determined either from the temperature dependence of the double exponential fit to the data (eq A8 of the appendix) or directly from the change in Bragg spacing with temperature at constant PEG stress using Maxwell relations as described in Leikin et al.[9] (and eq A4 of the appendix).

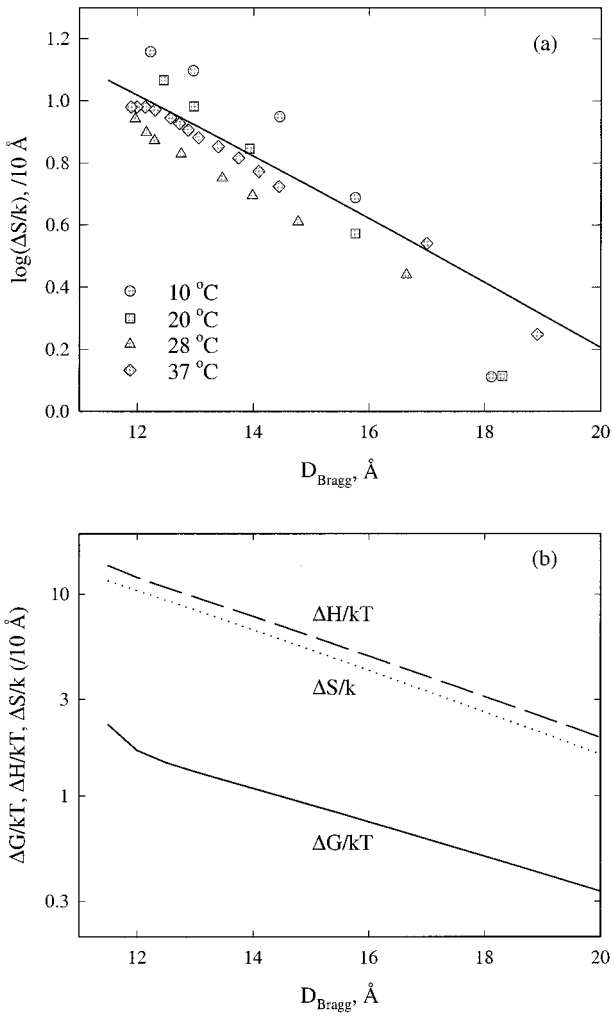

Figure 7. (a) Change in entropy per 10 Å length (approximately a disaccharide repeat distance) of the HPC phase as a function of the Bragg spacing. Entropy changes were calculated in two ways as described in the appendix. The solid line shows the entropy calculated (eq A8) from the temperature dependence of the longer ranged force amplitude, $B(T)$. The points show entropy changes calculated directly from the data at four temperatures using a Maxwell relation (eq A4) that relates the sensitivity of the Bragg spacing to temperature at constant PEG osmotic pressure to a change in entropy with PEG stress at constant temperature. The entropy itself appears to depend exponentially on distance with about the same decay length as the force. (b) The changes, expressed per 10 Å of polymer length, in entropy, enthalpy, and free energy at 20 °C, are shown vs the Bragg spacing of the HPC phase. The free energy was calculated from the Π-V work (eq A5), integrating the double-exponential fit. The entropy was calculated from the temperature derivative of the free energy as in (a). The enthalpy was calculated from $\Delta H/kT = \Delta G/kT + \Delta S/k$. The entropy and enthalpy are both much larger than the free energy. This "compensation" has sometimes been attributed to changes in solvation.

Figure 7a shows the entropy change associated with HPC dehydration as a function of Bragg spacing. The entropies calculated both directly from the data and from the temperature dependence of the double exponential fits are closely similar. Entropy increases as the HPC phase is concentrated. The entropy

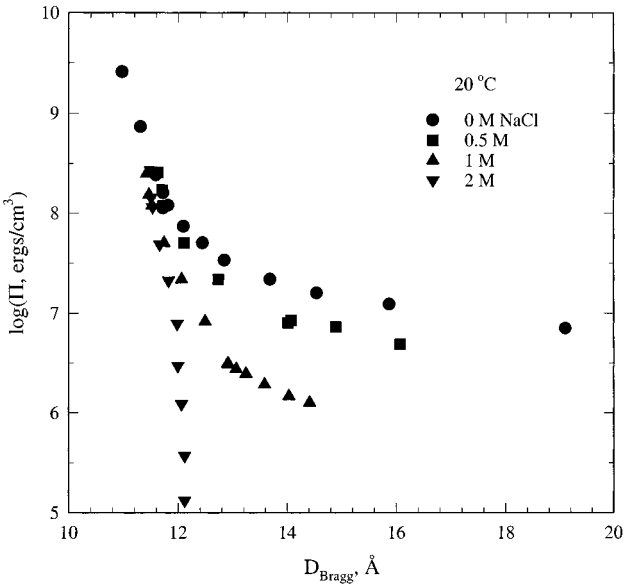

Figure 8. HPC force curves at 20 °C for different concentrations of NaCl (indicated in the figure). At a constant PEG stress, HPC molecules move closer as the salt concentration is increased. HPC will spontaneously precipitate at ~20 °C from dilute solution in 2 M NaCl.

varies approximately exponentially with about the same 4 Å decay length as seen in the force curves themselves. Figure 7b shows the variation of free energy, enthalpy, and entropy with D_{Br} at 20 °C. The change in Gibbs free energy is significantly smaller than changes in both the entropy and enthalpy that almost exactly cancel each other. Similar compensation between enthalpy and entropy has been observed previously with Mn^{2+} condensed DNA[19] and has often been associated with changes in hydration accompanying reactions or conformational changes.[20,21]

Effect of Salt. Despite the absence of charged groups on HPC (except for some infrequent oxidation products), salt strongly affects HPC interactions. Figure 8 shows Π-D_{Br} curves at 20 °C in 0, 0.5, 1, and 2 M NaCl. The apparent magnitude of the repulsion decreases as the salt concentration increases. HPC precipitates from 2 M NaCl solutions at room temperature without any added PEG, similar to the "salting-out" effect observed for many proteins (see, e.g., Collins and Washabaugh[22] and Cacace et al.[23]).

From simple thermodynamic considerations, this dependence of force on salt necessarily means a significant change in the salt concentration within the condensed phase as the HPC molecules move closer together (see appendix). We cannot determine from these data, however, whether there is a net inclusion or exclusion of salt from the macromolecular phase compared with the bulk solution. Both can account for the apparent weaker repulsion. Included salt may act through a direct effect on intermolecular interactions, e.g., screening of the electrostatic interactions between hydroxyl dipoles. Excluded salt applies its own osmotic stress, acting on the HPC phase in addition to that of the excluded PEG. Exclusion of salt or, equivalently, "preferential hydration"[24] of the HPC phase would result if the salt was simply too large to enter the confined spaces within the HPC array or if direct salt-HPC interactions were unfavorable.

To distinguish salt inclusion from exclusion, we have solvated dry HPC in salt solutions at 45 °C and monitored the resulting changes in salt concentration of the bathing solution using refractive index measurements. Table 1 shows the differences in the refractive indices of the bathing solution before and after

TABLE 1: Salt Preferentially Excluded from the Condensed HPC Phase[a]

g (2m NaCl)/g (dry HPC)	Δn	$[NaCl]_{final}$, m
2.0	0.002 ± 0.0005	2.22 ± 0.06
1.5	0.004 ± 0.0005	2.44 ± 0.06
1.0	0.0065 ± 0.0005	2.72 ± 0.06

[a] Dry HPC was hydrated in 2 molal NaCl at 45 °C at three weight ratios. HPC only swells to a Bragg spacing of ~12.4 Å under these conditions. The final concentrations of NaCl in the supernatants were determined from their refractive indices. Δn is the difference between the refractive index after equilibration and of the initial 2 molal NaCl solution. The refractive index difference between 2 m NaCl and water is 0.018. Refractive indices of these salt solutions vary linearly with concentration. As a control experiment, dry HPC was hydrated with water at 45 °C. No change in the refractive index was observed after equilibration, showing that no soluble components are present in the dry HPC that would affect the refractive index measurements.

hydrating dry HPC. The observed increase in the refractive index indicates an increase in NaCl concentration in the bathing solution. Salt is excluded from the condensed HPC sample that preferentially takes up water as it swells. As expected in this case, the change in the refractive index is approximately linear with increasing sample/solution ratio. The effect is significant. At a 1:1 sample/solution weight ratio, the concentration of salt in the bathing solution increases approximately 35%. Because we do not have an accurate measure of the total amount of water taken up by the samples, however, this measurement is only qualitative. If we assume a change in Bragg spacing from 10.9 to 12.5 Å with hydration at 45 °C in 2 M NaCl, a molecular weight of an hydroxypropyl glucose unit as 350, and a 5 Å repeat spacing per glucose unit along the polymer axis, then we can crudely estimate that the salt concentration within the condensed HPC phase is < 0.5 M.

If we assume that the effect of excluded salt is purely osmotic, the partitioning of salt can be quantitated from the dependence of the Π-D_{Br} curves on salt concentration. Specifically, we assume that NaCl does not directly affect interaction, structure, or conformation of HPC molecules. The only effect of NaCl then is that the total osmotic stress on the sample is the sum of the PEG and the excluded salt contributions, not just the PEG stress as plotted in Figure 8. The PEG stress is defined as the osmotic pressure of a PEG-salt solution relative to the reference solution with the same salt activity. The extra salt osmotic pressure, $\Delta\Pi_{NaCl}$, is then the difference in PEG osmotic pressures needed to attain the same Bragg spacing in the presence and absence of salt,

$$\Delta\Pi_{NaCl}(D_{Br},[NaCl]) = \Pi_{PEG}(D_{Br},0) - \Pi_{PEG}(D_{Br},[NaCl]) \quad (4)$$

This extra pressure cannot exceed the osmotic pressure of the corresponding salt solution relative to pure water, Π_{max}. Because the osmotic pressure of NaCl varies approximately linearly with salt concentration over the range investigated, the ratio of the measured excess pressure to the maximum possible salt pressure, $\Delta\Pi/\Pi_{max}$, reflects the excluded fraction of salt.

The excess pressure ratio is plotted in Figure 9 vs the Bragg spacing for several salt concentrations and temperatures. The normalized, excluded salt osmotic stress itself is surprisingly independent of the salt concentration and temperature and appears to vary exponentially with ~4 Å decay length. The salt exclusion is essentially complete ($\Delta\Pi/\Pi_{max} \sim 1$) at $D_{Br} \sim 12$ Å; while at 20 Å spacing only ~10% of the salt seems to be excluded.

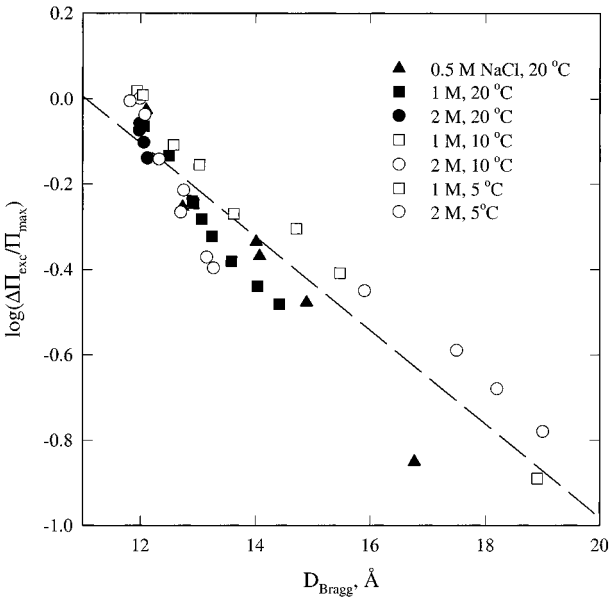

Figure 9. Apparent excess osmotic pressure from excluded salt acting on the HPC phase as a function of the Bragg spacing. The excess pressure due to salt exclusion is calculated as the difference between total pressure needed for the observed Bragg spacing without added salt and the PEG pressure with added salt, as described in the text (eq 4) and in the appendix. The excess salt stress is normalized by the total osmotic pressure of the salt solution. This pressure is the maximal stress the salt solution can apply, corresponding to complete exclusion. The different symbols represent different salt concentrations and temperatures as indicated in the figure. The exclusion of salt from HPC can be adequately described by an exponential function, as shown by the dashed line. The apparent exponential decay length (~3.8 ± 0.5 Å) is very similar to that for the force between HPC molecules.

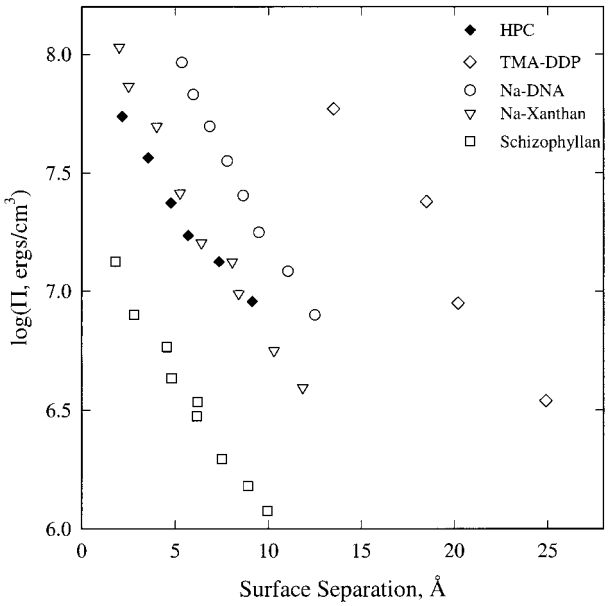

Figure 10. Comparison of the force curve measured here for HPC at 10 °C to the force curves previously measured for xanthan, schizophyllan, DNA, and didodecyl phosphate (DDP) bilayers. Interaxial spacings have been recalculated as distances between macromolecular surfaces. Xanthan, a bacterial polysaccharide, DNA, and DDP are charged; forces were measured in 0.4 M NaCl at 20 °C for xanthan and DNA and in 0.5 M TMACl at 20 °C for DDP bilayers. Schizophyllan, a fungal polysaccharide, and HPC are uncharged. The schizophyllan force curve was measured in in 1 mM TrisCl buffer at 20 °C. Although the force amplitude varies by almost 2 orders of magnitude between DDP bilayers and schizophyllan, the forces in all these systems appear to vary exponentially with surface separation with a common 3−4 Å decay length.

Discussion

Forces that Affect HPC Self-Assembly. Intermolecular forces appear to dominate HPC self-assembly; changes in configurational entropy have surprisingly little or no effect. The traditional starting point for theories of self-assembly or macromolecular compaction is to consider a balance of soft potential, attractive forces between polymers and the configurational entropy of the polymer. This approach typically predicts that higher temperatures favor the dissociated or open state that maximizes the entropy of the macromolecule. The assembly of hydroxypropylcellulose, however, does not fit within this simple framework. The temperature dependence of the measured forces indicates that the entropy of the whole condensed phase *decreases* as HPC molecules move apart, at least out to a Bragg separation of ~ 20 Å. From the sign of the entropy alone, we conclude that the measured force at spacings larger than about 12.5 Å cannot be due to steric, hard shell interactions associated with configurational freedom and motions of the polymer that would result in *increasing* entropy as the polymers move apart.

Furthermore, the intermolecular force measured in the very concentrated, condensed phase changes its sign from repulsion to attraction very close to the temperature at which polymer precipitation occurs from very dilute solution (~40 vs ~42 °C). This is even stronger evidence that the phase behavior is dominated by nonsteric, soft potential interactions with surprisingly little contribution from traditional configurational entropy. It is the change in force with temperature between molecules that drives the self-assembly even from dilute solution. The continued decrease in the Bragg spacing with no applied PEG stress as the temperature increases above ~40 °C (Figure 4 inset) indicates that the amplitude of this attraction continues to increase even up to 70 °C.

Forces that May Contribute to the Measured Net Interaction. Besides the hard shell steric repulsive forces associated with reduced configurational entropy at close spacings, a number of other forces can contribute to the net interaction seen in Figures 3 and 4. These include: direct hydrogen bonding of polysaccharide hydroxyls; dipolar interactions; van der Waals forces; and hydration/solvation interactions, the energies associated with removing solvent organized around polar or nonpolar groups. Steric interactions are purely repulsive. Direct hydrogen bonding, van der Waals forces between like objects, and hydrophobic (hydration) interactions between nonpolar residues are purely attractive. Dipolar interactions have attractive (dipole−dipole) and repulsive (dipole−image) components. Hydration interactions between polar residues can be either repulsive or attractive, depending on the complementarity of the surfaces.[9]

A remarkable feature of the measured HPC force−distance curves is their close similarity to the curves observed for many other, very different macromolecular systems. In Figure 10, the longer range force for HPC at 10 °C is compared with the force curves for the polysaccharides schizophyllan and xanthan,[25] for DNA,[26−28] and for didodecyl phosphate (DPP) bilayers.[29] The striking similarity of forces between surfaces that can be highly charged (xanthan, DNA, and DDP) or completely uncharged (HPC and schizophyllan) suggests a common origin for the ~3−4 Å decay length exponential repulsion.

We have argued previously that these forces reflect the energetic cost of removing water organized around polar groups on molecular surfaces. The theoretical frameworks for "hydration/solvation forces" are still primitive.[9,23,30−32] These interac-

tions are postulated to reflect the changes in water structuring between macromolecular surfaces as they approach. The amplitude of the force depends both on the interaction "strength" of water with a surface and on the mutual structuring of water on apposing surfaces. The ~ 4 Å decay length is tentatively associated with the length scale for water−water interactions. This length is consistent, for example, with the correlation length of density fluctuations in water estimated from X-ray diffraction.[33] It should be noted, however, that there is little evidence directly connecting water structuring and forces.[15,34] The consistency and the similarity of the forces in the different systems could be simply coincidental. There is, as yet, no broad agreement among different authors on the interpretation of the observed forces (see, for example, recent reviews[35,36]).

The much shorter ranged, temperature insensitive force that also seems to vary exponentially over the last 2 Å of separation but with a decay length of about 0.25 Å could certainly be due to hard-shell steric interactions between hydroxypropyl groups. Similar, very short decay length forces have been observed with lipid bilayers and attributed to steric interactions between headgroups.[37,38] Much shorter decay lengths, however, are also predicted for the hydration force equivalent of electrostatic image charge repulsion.[31,39] Decay lengths much shorter than the commonly observed 3−4 Å have been observed in a number of systems at very close spacings and seem attributable to a residual image charge class of interactions.[9,40] The energetic cost of removing the last few water molecules from between HPC molecules could well be very different from the predictions of mean-field hydration force theories and is another factor that should be considered.

Interactions with Salt. The effect of salt on forces between HPC molecules seen in Figure 8 is quite remarkable and unexpected for an uncharged polymer. The change between 0.5 and 2 M NaCl is far more dramatic for uncharged HPC than for very highly charged DNA.[26,27,41] Salt concentration insensitive hydration forces appear to overwhelm the electrostatic repulsion between DNA helices at high pressures and close spacings. Even at lower pressures and greater spacings, the effect of salt on DNA forces is most pronounced at salt concentrations less than ~0.5 M. The experiments hydrating dry HPC samples in salt solutions (Table 1) show that salt is excluded from the polysaccharide phase and, therefore, applies its own osmotic stress on the condensed HPC phase. This is equivalent to depletion forces that have been observed in colloidal systems.[42,43] The excess salt pressure (Figure 9) varies approximately linearly with salt concentration and exponentially with Bragg spacing with a decay length that is about the same for as the intermolecular force.

Although we cannot discount completely that salt exclusion is simply a size effect, the similarity between the distance dependence of the extra osmotic stress due to excluded salt and the long-ranged force between HPC molecules, in particular, and between many macromolecules, in general, suggests that hydration forces dominate the interaction of salt with HPC. In the same way that the structuring of water on one macromolecule can perturb the water structuring of an apposing macromolecular surface creating repulsive forces, small solutes can also interact with macromolecules through perturbations in hydration. In this case, however, repulsive interactions mean an exclusion of salt from the macromolecular surface. An exclusion of NaCl from the HPC phase through hydration forces would indicate that the water structuring around these ions is less compatible with the water organization near the polysaccharide surface than in the bulk solution.

Because different ions structure water differently, one obvious strategy for further probing the interaction of salt with the HPC surface is to correlate the magnitude of the effect with the nature of the salt species, for example, within the Hofmeister series. Indeed, the cloud point temperature for the precipitation of HPC from dilute solution depends not only on salt concentration but also on salt species.[44] At the same salt concentration, the transition temperature is significantly lower with NaF or KF than with NaCl or KCl, which in turn is more effective than either KBr or KSCN. The observation of hydration forces acting between salts and HPC would provide a direct link between Hofmeister effects and water structuring, elucidating the mechanism of protein salting out[22] and the general phenomenon of preferential hydration of macromolecular surfaces.[24]

Attractive Force; Possible Origins of the Entropy. We do not know which groups on HPC are responsible for the attraction between polymers. The stereospecific arrangement of hydroxyl groups on cellulose itself underlies the extensive H-bond network between polymers in the fiber. Changing either the type of sugar or the linkage between them weakens or destroys this complementarity. It is possible that favorable H-bonding interactions between OH groups on hydroxypropyl-modified cellulose (either direct or mediated by water) are similarly responsible for the assembly of HPC. Alternatively, it is also possible that assembly is due to attractive hydrophobic interactions between the propyl groups and that solvated hydroxyl groups resist compaction. Increased hydrophobic substitution of cellulose does typically result in lower cloud point transition temperatures.[3] The physics behind the "hydrophobic bond" is not well understood. It is thought that the release of water structured around nonpolar groups is an important contributor to the energetics of the hydrophobic bond formation. A dominating hydrophobic effect is also consistent with strong exclusion of salt from HPC. Salt is known to lower the solubility of nonpolar molecules.[45]

Qualitatively similar, temperature dependent exponential force curves have been measured for Mn^{2+}−DNA[19,46] and for collagen,[12,47] both of which also show increased attraction and assembly with increased temperature. For all three systems, condensed array forces show a balance between an apparent short-ranged (small decay length) exponential repulsion and a longer ranged force that also seems to be exponential. For all three, the amplitude of the short-ranged repulsion is temperature insensitive, whereas the longer-ranged force becomes more attractive with increasing temperatures. For both HPC and Mn^{2+}−DNA, there is a clear transition from a net long-range repulsion to a net attraction at some critical temperature. For all three systems, equilibrium spacings between spontaneously assembled macromolecules without applied osmotic stress decrease as the temperature is raised. Figure 5 suggests that for HPC there is only one longer range exponential force whose temperature dependent amplitude gradually changes from repulsion to attraction with increasing temperature.

The temperature dependence of the force curves can be transformed directly into an entropy change with varying separation between the surfaces, as briefly discussed in the appendix and in Leikin et al.[19] The entropy vs Bragg spacing curves obtained by two different methods for HPC are shown in Figure 7a. The apparent ~4 Å decay length exponential is remarkably similar to the entropy vs separation curve found for Mn^{2+}−DNA assembly.[19]

Two classes of theories have been proposed to account for the connection between the entropy and attractive forces. In one model, the entropy would result from the increased freedom of

groups on the HPC surface.[48] With isolated surfaces, the freedom of motion is determined by widths of local energy minima. If the local minimum is not optimal for an attractive interaction between groups on apposing surfaces, then the surface rearrangement that minimizes free energy must necessarily also increase the range of motion of groups on the surface. In essence, the width of the energy minimum restricting motion increases due to the attraction between groups.

Alternatively, the increased entropy accompanying the assembly of HPC could come from the increased freedom of water released from around HPC. It is postulated that the water organized either around nonpolar moieties (the hydrophobic effect) or around polar residues of HPC is more structured and has lower entropy than water in the bulk solution. No enhanced motion of surface groups or surface waters must be presumed. Since the net force may reflect a balance between attractive hydrophobic interactions and repulsive hydration forces between hydrophilic groups, a difference in the temperature sensitivity of structuring water around hydrophobic and hydrophilic groups can also result in temperature-dependent forces.

These possibilities are, of course, not mutually exclusive; both may contribute to the observed temperature dependence and the entropy change. Yet other models may eventually prove preferable. We can measure the total entropy vs distance between the molecules as shown in Figure 7a, but we cannot distinguish different contributions experimentally. Direct experimental probes of side chain and backbone motions and of water ordering as dependent on spacing are needed to complement the entropy measurements.

Concluding Remarks

We are now seeing a remarkable coincidence of measured forces that depend exponentially on distance with a characteristic 3−4 Å decay length. With the HPC data, this force has now been measured between nonpolar polymers as well as between highly polar, even charged macromolecules. Furthermore, the dependence of entropy on intermolecular spacing extracted from temperature dependent force curves measured for self-assembling HPC polymers is similar not only to the force dependence but also to the entropy−distance dependence measured for a very different, self-assembling system, Mn^{2+}−DNA helices. Finally, the same force appears to dominate the interaction of salt with HPC. A hydration force still seems the most reasonable explanation for these recurring observations on quite disparate systems. The results specifically suggest a close connection between the interactions of hydrophilic surfaces and the hydrophobic bond. Perhaps these force measurements on HPC and future measurements on other polymers and surfaces, both closely related in structure and composition and of considerably different chemistry, will begin to link these two forces that are so critical to understanding the structure and interactions of molecules in aqueous solution, particularly in biochemistry and biology.

Appendix

Thermodynamics of Hydroxypropylcellulose Hydration. *(1.) Temperature − Entropy.* The change in work done on HPC to bring it from one degree of hydration to another under a change in osmotic stress or a change in temperature is

$$\mathrm{d}G(T, \Pi_{osm}) = -S(T, \Pi_{osm})\,\mathrm{d}T + V_w(T, \Pi_{osm})\,\mathrm{d}\Pi_{osm}$$

In fact, the measurement of the volume $V_w(T, \Pi_{osm})$ of water is through the measured Bragg spacing $D_{Br}(T, \Pi_{osm})$ where the volume of HPC and water per disaccharide unit of length l (∼10 Å) is

$$V = V_{HPC} + V_w(T, \Pi_{osm}) = \alpha\, l D_{Br}^{\,2} \tag{A1}$$

or

$$\mathrm{d}V = \mathrm{d}V_w(T, \Pi_{osm}) = 2\alpha\, l D_{Br}\, d\mathrm{D}_{Br} \tag{A2}$$

The factor α depends on the packing symmetry. For simplicity we take α = 1, not very different from the $2/\sqrt{3}$ factor that it would be if HPC packing were to have hexagonal symmetry.

Because $G(T, \Pi_{osm})$ is a state function, it is possible to use a Maxwell cross relation to compute the change in S with osmotic stress from the observed change in V_w with temperature

$$\left.\frac{\partial S}{\partial \Pi_{osm}}\right|_T = -\left.\frac{\partial V_w}{\partial T}\right|_{\Pi_{osm}} \approx -\left.\frac{21 D_{Br}\partial D_{Br}}{\partial T}\right|_{\Pi_{osm}} \tag{A3}$$

The entropy change can be calculated from the measured dependence of $(\partial D_{Br}/\partial T)|_\Pi$ on Π_{osm}.

$$\Delta S = \int \left.\frac{\partial \mathrm{S}}{\partial \Pi_{osm}}\right|_T \mathrm{d}\Pi_{osm} \approx \int -\left.\frac{2 l D_{Br}\partial D_{Br}}{\partial \mathrm{T}}\right|_{\Pi_{osm}} \mathrm{d}\Pi_{osm} \tag{A4}$$

A more detailed discussion is given in Leikin et al.[19]

Alternatively, since the free energy can be straightforwardly calculated as a $\Pi_{osm} - V_w$ work of dehydrating HPC from $D_{Br} = \infty$ to D,

$$\Delta G_{HPC}(\infty \rightarrow \mathrm{D}) = -\int_\infty^D \Pi_{osm}(D_{Br}, T)\,\mathrm{d}V_w \tag{A5}$$

the entropy change can be determined from the temperature derivative of the free energy change at constant hydrostatic pressure,

$$\Delta S = -\frac{\partial \Delta G_{HPC}}{\partial \mathrm{T}} = \frac{\partial}{\partial T}\int_\infty^D \Pi_{osm}(D_{Br}, T)\,\mathrm{d}V_w \approx \frac{\partial}{\partial T}\int_\infty^D \Pi_{osm}(D_{Br}, T) 2 l D_{Br}\,\mathrm{d}D_{Br} \tag{A6}$$

We can use the double exponential function fitted to the data for $\Pi_{osm}(D_{Br}, T)$,

$$\Pi_{osm}(D_{Br}, T) = \mathrm{A}e^{-(D_{Br}-D_0)/\lambda_1} + \mathrm{B}(T)e^{-(D_{Br}-D_0)/\lambda_2} \tag{A7}$$

to evaluate the entropy change in dehydrating HPC from $D_{Br} = \infty$ to D,

$$\Delta S(\infty \rightarrow D) = -2l\frac{\mathrm{d}B(T)}{\mathrm{d}T}\lambda_2(\lambda_2 + D)e^{-(D-D_0)/\lambda_2} \tag{A8}$$

The double exponential fit can also be used to calculate the free energy change from eq A5. The enthalpy change of dehydration is then

$$\Delta H = \Delta G + T\Delta S \tag{A9}$$

(2) Salt Exclusion − $\Pi_{exc.}$ There are several ways to approach the problem of the additional osmotic stress exerted by excluded salt in addition to that of the stressing polymer, typically PEG. One of the simplest is to model the action of PEG as a piston applying a pressure Π_{PEG} on a semipermeable membrane that separates the HPC phase from a reference salt solution, as was developed in Leikin et al.[19] This separation assumes that the salt does not affect significantly the contribution of PEG to the

osmotic pressure. Because the osmotic pressures of NaCl and PEG are approximately additive over the range of concentrations used, we assume this condition is satisfied. If the HPC phase contains N_s and N_w molecules of salt and water per HPC unit, then at constant temperature and hydrostatic pressure the Gibbs−Duhem equation is

$$dG_{HPC} = -N_s\, d\mu_s - N_w\, d\mu_w \tag{A10}$$

In terms of the reference solution and PEG piston,

$$d\mu_s = d\mu_s^{ref} \text{ and } d\mu_w = d\mu_w^{ref} - \bar{v}_w\, d\Pi_{PEG} \tag{A11}$$

where $\bar{v}_w$ is the volume of a water molecule. The chemical potentials of the salt and water in the reference phase containing n_s and n_w salt and water molecules, respectively, are themselves related by a Gibbs−Duhem relation for the reference solution.

$$d\mu_s^{ref} = -(n_w/n_s)\, d\mu_w^{ref} \tag{A12}$$

Combining these equations, we have where $V_w = \bar{v}_w N_w$. The

$$\begin{aligned} dG_{HPC} &= V_w d\Pi_{PEG} - N_w\left(1 - \frac{(N_s/N_w)}{(n_s/n_w)}\right) d\mu_w^{ref} \\ &= V_w\left(d\Pi_{PEG} + \left(1 - \frac{(N_s/N_w)}{(n_s/n_w)}\right) d\Pi_{ref}\right) \end{aligned} \tag{A13}$$

excess stress applied by the salt is therefore

$$d\Pi_{exc} = \left(1 - \frac{(N_s/N_w)}{(n_s/n_w)}\right) d\Pi_{ref} \tag{A14}$$

The magnitude of the extra salt pressure depends on the ratio of the salt concentrations in the HPC and reference phases, $(N_s/N_w)/(n_s/n_w)$. If there is no difference in concentration between the two phases ($N_s/N_w = n_s/n_w$), then there is no extra stress applied by the salt. If, like PEG, the salt is also completely excluded from the HPC phase ($N_s/N_w = 0$), then the maximal, excess stress is the total osmotic pressure of the reference salt solution, Π_{ref}.

If there is no interaction of the salt other than exclusion (as, for example, direct binding to HPC), the excess pressure due to the excluded salt, Π_{exc}, can be calculated through an integrated form of the above equation. If $\Pi_{PEG}(D_{Br}, c_s)$ and $\Pi_{PEG}(D_{Br}, 0)$ are the osmotic stresses due to PEG at a spacing D_{Br} with and without added salt at a concentration c_s, then

$$\frac{\Pi_{exc}(c_s)}{\Pi_{ref}(c_s)} = \frac{\Pi_{PEG}(D_{Br}, c_s) - \Pi_{PEG}(D_{Br}, 0)}{\Pi_{ref}(c_s)} = 1 - \frac{(N_s/N_w)}{(n_s/n_w)} \tag{A15}$$

The excess pressure is a direct measure of the salt distribution surrounding HPC.

References and Notes

(1) Just, E. K.; Majewicz, T. G. *Encyclopedia of Polymer Science and Engineering*, 2nd ed.; Wiley: New York, 1985; Vol 3, 226.

(2) Sandford, P. A.; Baird, J. *The Polysaccharides*; Aspinall, G. O., Ed.; Academic Press: Orlando, 1983; Chapter 7.

(3) Klug, E. D. *J. Polymer Sci. Part C* **1971**, *26*, 491.

(4) Werbowyj, R. S.; Gray, D. G. *Macromolecules* **1980**, *13*, 69.

(5) Winnik, F. M. *Macromolecules* **1987**, *20*, 2745.

(6) Fortin, S.; Charlet, G. *Macromolecules* **1989**, *22*, 2286.

(7) Guido, S. *Macromolecules* **1995**, *28*, 4530.

(8) Parsegian, V. A.; Rand, R. P.; Fuller, N. L.; Rau, D. C. *Methods Enzymol.* **1986**, *127*, 400.

(9) Leikin, S.; Parsegian, V. A.; Rau, D. C.; Rand, R. P. *Annu. Rev. Phys. Chem*. **1993**, *44*, 369.

(10) Parsegian, V. A.; Evans, E. A. *Curr. Opin. Colloid Interface Sci*. **1996**, *1*, 53.

(11) Strey, H. H.; Podgornik, R.; Rau, D. C.; Parsegian, V. A. *Curr. Opin. Struct. Biol*. **1998**, *8*, 309.

(12) Leikin, S.; Rau, D. C.; Parsegian, V. A. *Nature Struct. Biol*. **1995**, *2*, 205.

(13) O'Brien, F. E. M. *J. Scientific Instrum*. **1948**, *25*, 73.

(14) Mudd, C. P.; Tipton, H.; Parsegian, V. A.; Rau, D. C. *Rev. Sci. Instrum*. **1987**, *58*, 2110.

(15) Kuznetsova, N.; Rau, D. C.; Parsegian, V. A.; Leikin, S. *Biophys. J*. **1997**, *72*, 353.

(16) Vainshtein, B. K. *Diffraction of X-rays by Chain Molecules*; Elsevier: New York, 1966.

(17) Helfrich, W.; Harbich, W. *Chem. Scr*. **1985**, *25*, 32.

(18) Selinger, J. V.; Bruinsma, R. F. *Phys. Rev. A* **1991**, *43*, 2910.

(19) Leikin, S.; Rau, D. C.; Parsegian, V. A. *Phys. Rev. A* **1991**, *44*, 5272.

(20) Grunwald, E.; Steel, C. *J. Am. Chem. Soc*. **1995**, *117*, 5687.

(21) Qian, H.; Hopfield, J. J. *J. Chem. Phys*. **1996**, *105*, 9292.

(22) Collins, K. D.; Washabaugh, M. W. *Quart. Rev. Biophys*. **1985**, *18*, 323.

(23) Cacace, M. G.; Landau, E. M.; Ramsden, J. J. *Quart. Rev. Biophys*. **1997**, *30*, 241.

(24) Timasheff, S. N. *Annu. Rev. Biophys. Biomol. Struct*. **1993**, *22*, 67.

(25) Rau, D. C.; Parsegian, V. A. *Science* **1990**, *249*, 1278.

(26) Rau, D. C.; Lee, B.; Parsegian, V. A. *Proc. Natl. Acad. Sci. U.S.A.* **1984**, *81*, 2621.

(27) Podgornik, R.; Rau, D. C.; Parsegian, V. A. *Biophys. J*. **1994**, *66*, 962.

(28) Podgornik, R.; Strey, H. H.; Gawrisch, K.; Rau, D. C.; Rupprecht, A.; Parsegian, V. A. *Proc. Natl. Acad. Sci U.S.A.* **1996**, *93*, 4261.

(29) Fang, Y.; Rand, R. P.; Leikin, S.; Kozlov, M. M. *Phys. Rev. Lett*. **1993**, *70*, 3623.

(30) Marcelja, S.; Radic, N. *Chem. Phys. Lett*. **1976**, *42*, 129.

(31) Leikin, S.; Kornyshev, A. A. *J. Chem. Phys*. **1990**, *92*, 6890.

(32) San Biagio, P. L.; Bulone, D.; Martorana, V.; Palma-Vittorelli, M. B.; Palma, M. U. *Eur. J. Biophys*. **1998**, *27*, 183.

(33) Xie, Y.; Ludwig, K. F., Jr.; Morales, G. *Phys. Rev. Lett*. **1993**, *71*, 2050.

(34) Leikin, S.; Parsegian, V. A.; Yang, W.-H.; Walrafen, G. E. *Proc. Natl. Acad. Sci. U.S.A.* **1997**, *94*, 11312.

(35) McIntosh, T. J.; Simon, S. A. *Annu. Rev. Biophys. Biomol. Struct*. **1994**, *23*, 27.

(36) Israelachvili, J.; Wennerstrom, H. *Nature* **1996**, *379*, 219.

(37) McIntosh, T. J.; Magid, A. D.; Simon, S. A. *Biochem*. **1987**, *26*, 7325.

(38) McIntosh, T. J.; Magid, A. D.; Simon, S. A. *Biochem*. **1989**, *28*, 17.

(39) Kornyshev, A. A.; Leikin, S. *J. Chem. Phys*. **1997**, *107*, 3656.

(40) Kornyshev, A. A.; Leikin, S. *Biophys. J*. **1998**, *75*, 2513.

(41) Podgornik, R.; Rau, D. C.; Parsegian, V. A. *Macromolecules* **1989**, *22*, 1780.

(42) Asakura, S.; Oosawa, F. *J. Polym. Sci*. **1958**, *33*, 183.

(43) Singh-Zocchi, M.; Andreasen, A.; Zocchi, G. *Proc. Natl. Acad. Sci. U.S.A.* **1999**, *96*, 6711.

(44) Chik, J. K.; Rau, D. C.; Parsegian, V. A. *Biophys. J*. **1999**, *76*, A320.

(45) Long, F. A.; McDevit, W. F. *Chem. Rev*. **1952**, *51*, 119.

(46) Rau, D. C.; Parsegian, V. A. *Biophys. J*. **1992**, *61*, 260.

(47) Leikin, S.; Rau, D. C.; Parsegian, V. A. *Proc. Natl. Acad. Sci. U.S.A.* **1994**, *91*, 276.

(48) Leikin, S.; Parsegian, V. A. *Proteins: Struct. Func. Genet*. **1994**, *19*, 73.